Anisa Isabella

by Samuel Kusumocahyo

Submission date: 21-Jan-2020 04:06PM (UTC+0700)
Submission ID: 1244370846
File name: 2019_IOP_Proceedings_sol_gel_synthesis.pdf (1.36M)
Word count: 3527
Character count: 19200

Sol-gel method for synthesis of Li^+-stabilized Na-β"-alumina for solid electrolytes in sodium-based batteries

Cite as: AIP Conference Proceedings **2175**, 020070 (2019); https://doi.org/10.1063/1.5134634
Published Online: 20 November 2019

Anisa I. Agustina, Karl Skadell, Cornelius L. Dirksen, Matthias Schulz, and Samuel P. Kusumocahyo

Sol-Gel Method for Synthesis of Li^+-Stabilized Na-β"-Alumina for Solid Electrolytes in Sodium-Based Batteries

Anisa I. Agustina[1], Karl Skadell[2], Cornelius L. Dirksen[2], Matthias Schulz[2], and Samuel P. Kusumocahyo[1,a)]

[1]*Department of Chemical Engineering, Swiss German University, The Prominence Tower Alam Sutera, Tangerang 15143, Indonesia*

[2]*Fraunhofer Institute for Ceramics Technologies and Systems IKTS, Hermsdorf 07629, Germany.*

[a)]Corresponding author: samuel.kusumocahyo@sgu.ac.id

Abstract. Li^+-stabilized Na-β"-alumina was synthesized through sol-gel based on the *Pechini* method with $Al(NO_3)_3$, $NaNO_3$, and $LiNO_3$ as the metal precursor. Evaluations were done to several different sodium content in order to counterbalance Na_2O losses during sintering, as well as different sintering temperature between 1500 – 1700 °C. The evaluations were done by density measurement, impedance spectroscopy, X-ray diffraction, and Scanning Electron Microscopy. The synthesized powder exhibits Na-β alumina with measured relative density up to 2.96 ± 0.01 g/cm^3. The ionic conductivity achieved was up to 0.23 S/cm at 300 °C with lowest activation energy for conduction of 0.17 eV. Moreover, the Na-β"-alumina phase content achieved was up to 84%.

INTRODUCTION

Economic and population growth intensively increased the energy consumption, which is still dominantly fulfilled by conventional energy sources. The depletion of fossil fuel and its environmental concerns drive the need for renewable energy production, such as solar and wind energy. However, renewable energy productions are fluctuating due to unpredictable natural force that could limit the energy generation. Stationary energy storage has been used to cope with energy variability problem main bound to variable renewable energy, that allows the possibility to provide excess energy during peak times as their appearances are fluctuating.

Low cost, easy extractability, and abundance of sodium resources in contrast to lithium and cobalt, make sodium-based rechargeable batteries, such as Na/S or Na/$NiCl_2$ battery, as an ideal type for large-scale production [1], [2]. The key component of sodium-based batteries is Na-β"-alumina solid electrolyte, due to its high sodium ion conductivity and electrical insulating properties [3]. Typically, Na-β"-alumina exhibits ionic conductivity of 0.2-0.4 S cm^{-1} at 300 °C [4]. Moreover, the use of solid electrolyte minimizes the potential of leaking and explosion hazard in comparison to utilization of solvent-based electrolytes. Processing fine Na-β"-alumina has been reviewed, as nano-particles has higher sodium ion conductivity compared to micro-sized particles [5]. Conventionally, Na-β"-alumina is synthesize by solid-state reaction of boehmite, Na_2CO_3, and a small amount of magnesium or lithium oxide [6]. However, solid-state method has the main disadvantage of inhomogeneity of the starting materials and requirement of repetitive grinding, compaction, and annealing which results in high cost and energy consumption [7].

Interest has grown towards the use of citrate sol-gel as an alternative method as it has an advantage of molecular-level mixing which could increase the homogeneity of the materials [5], [7]. The *Pechini* method was established by involving chelating agent to form homogeneous dispersed solution of metal/citrate complexes [8]. The complexes are further converted into a polymer network with gel as an intermediate product. Li^+ or Mg^{2+} doping stabilizes the crystal structure while sintering Na-β"-alumina ceramic [9], [10]. A composition of $Na_{1.67}Li_{0.33}Al_{10.67}O_{17}$ is an ideal stoichiometric as the optimum composition of Li^+-stabilized Na-β"-alumina [9]. However, the sodium content should be elevated to counterbalance the Na_2O losses during calcination and sintering [11]. The typical sintering temperature

Proceedings of the 5th International Symposium on Applied Chemistry 2019
AIP Conf. Proc. 2175, 020070-1–020070-8; https://doi.org/10.1063/1.5134634
Published by AIP Publishing. 978-0-7354-1922-3/$30.00

of Na-β"-alumina is 1600 °C [7], [9], [12]. In this study, Li^+-stabilized Na-β"-alumina was synthesized through sol-gel based on *Pechini* method using metal nitrates, citric acid, and ethylene glycol as the reaction fuel. The prepared Na-β"-alumina were studied regarding its density, conductivity, phase analysis, and microstructure to determine the optimal sintering temperature and sodium content in the precursor.

EXPERIMENTAL PROCEDURUE

Sample preparation

Na-β"-alumina was synthesized through sol-gel route based on the *Pechini* method using $Al(NO_3)_3.9H_2O$ (Carl Roth, 99.5%), $NaNO_3$ (VWR, 99%), $LiNO_3$ (VWR, 99%), citric acid (Carl Roth, 99.5%), and ethylene glycol (Carl Roth). In the first step, variations of metal precursor stoichiometric amounts ($Na_{1.67}Li_{0.33}Al1_{0.67}O_{17}$, $Na_{1.71}Li_{0.33}Al1_{0.67}O_{17}$, and $Na_{1.75}Li_{0.33}Al1_{0.67}O_{17}$) were dissolved in distilled water. Then citric acid and ethylene glycol solution were added into the prepared solution with different molar ratio of metallic ions, citric acid, ethylene glycol of 1:2:1 were obtained. The resulting mixture was undergone aging process by slowly evaporated at temperature of 80 °C while stirring in a water bath until a yellow colored transparent gels were formed. The viscous gel was transferred into pre-heated muffle furnace and was dried at 120 °C. Subsequently, the powder was obtained by ball-milling foamy product obtained after drying process. The obtained powder was calcined in a high-temperature muffle furnace at 1200 °C. The calcined powder was granulated by mixing the powder with organic binding agent. The granules were sieved to obtain particle size in the range of 100-400 µm. The granules were uniaxially pressed (100 kN load) into bars (6 x 6 x 60 mm). The bars were sintered for 30 minutes under dense MgO crucibles at three different temperatures of 1500, 1600, and 1700 °C.

Characterization methods

The bars were cut into pieces with length of around 20 mm and used for density and ionic conductivity measurements. Density measurements were carried out based on Archimedes' principle in toluene. The ionic conductivity measurements were done by Impedance spectroscopy (BioLogic SP-240 and Gamry Reference 3000 AE) at temperature of 240 to 330 °C. The sintered bar was clamped between two nickel-plated aluminium sample holder (**Fig.1**), which are each provided with Promat glass fiber paper (Promaglav HTI 1250 with diameter of 12 mm) and impregnated with ± 0.05 g of salt mixture (7 wt.% $NaNO_3$, 50 wt.% $NaNO_2$, and 43 wt.% KNO_3). The applied frequencies was in the range between 1 MHz to 10 Hz. The specific conductivity was calculated by Eq.1 where L represents the length of the sample and A the cross-sectional area.

$$\sigma = \frac{L}{A\,R} \tag{1}$$

The resistance of the sample (R) was calculated by selecting the bulk- (R_b) and the grain boundary resistance (R_{gb}) from regression analysis curve. Moreover, temperature dependance of ionic conductivity were analyzed based on Arrhenius' equation (Eq.2).

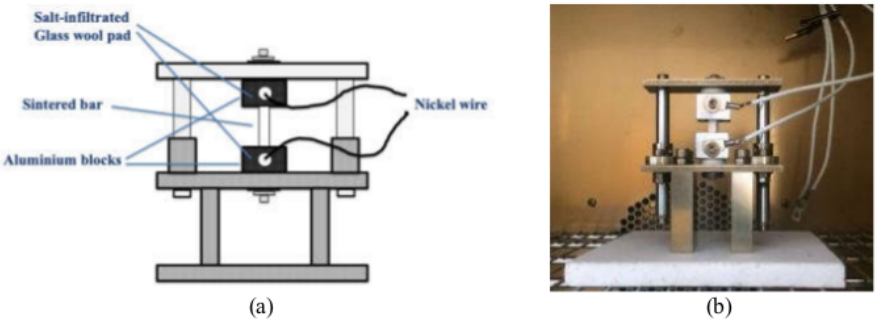

(a) (b)

FIGURE 1. Sketch (a) and picture (b) of sample assembling in cell measurement device for ionic conductivity measurement.

$$\sigma = \frac{\sigma_0}{T}\exp\frac{-E_a}{k\,.\,T} \tag{2}$$

Where σ is conductivity in S cm^{-1}, σ_0 is the pre-exponential constant, T is temperature in Kelvin (K), E_a is activation energy in eV, and k is the Boltzman constant in eV K^{-1}. Activation energy was calculated using slope from ln(σT) over 1000 T^{-1} axis.

X-ray diffraction patterns (D8 Advance, Bruker, USA) were taken from ball-milled bars. The diffraction patterns were analyzed quantitatively by Rietveld refinement method (AutoQuan 2.8.0.2). SEM micrographs (Zeiss Ultra 55+, Germany) were recorded on a perpendicular fracture surface of the sintered bars. The fracture surface was carbon coated to improve the electron signal by creating conductive layer.

RESULTS AND DISCUSSION

(a) (b) (c)

FIGURE 2. (a) Xerogel formed after drying process. (b) Carbon trapped in MgO crucible during calcination. (c) Agglomeration of calcined powder.

During sample preparation, white yellowish foamy structure with significant expansion phenomenon after drying process was observed (**Fig.2a**). The expansion was formed as NOx gasses trapped in the solution. Subsequently, the powder was obtained by dry ball-milling the foamy structure and was calcined at 1200 °C. During calcination, carbon was trapped in the MgO crucible as the cap was tightly closed (**Fig.2b**). Moreover, it might also happen due to insufficient of oxygen during calcination, as the sample contained organic materials. To prevent this phenomenon, the MgO crucible can be slightly open during the calcination process. The change of powder color from gray to white indicates the complete removal of carbon (**Fig.2c**).

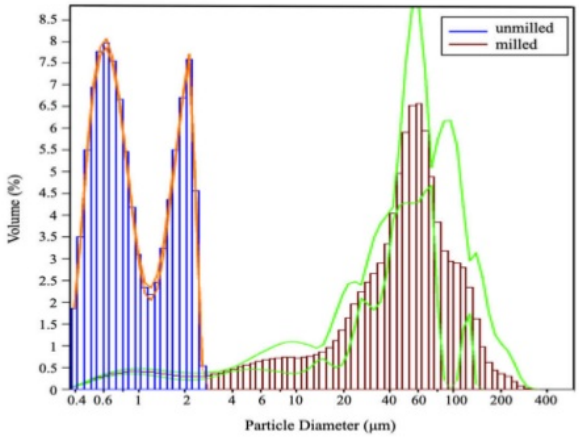

FIGURE 3. Particle size distribution of calcined powder before and after dry ball-milling.

The particles were agglomerated after calcination with a significant volume reduction, as the organic compounds were removed. The agglomerated calcined powder requires ball-milling to reduce the particle size. The particle size distributions were shown in **Fig.3**. The measurement was done three times each for sample (with and without milling). Red and green lines are representing each measurement, while the blue and red bar diagram shows the average of the measurement. Without milling, bigger particle size with distribution in a range of 40-100 µm were dominant. Smaller particle size was also present with a low vol.% compared to bigger particles. With milling, it can be seen that significant particle size reduction was achieved, as the particles was milled properly and the size present was < 3 µm.

Density Analysis

In **Fig.4,** the relative density of Na-β”-alumina ceramic samples with different sodium content are plotted against sintering temperature of 1500, 1600, and 1700 °C. During relative density measurement, air bubbles were present when samples sintered at 1500 °C were submerged into toluene. These phenomena show that these samples are porous, which also in accordance with **Fig.4** as samples sintered at 1500 °C have relatively low density. Samples with low and high sodium content ($Na_{1.67}Li_{0.33}Al_{10.67}O_{17}$ and $Na_{1.75}Li_{0.33}Al_{10.67}O_{17}$, respectively) show a same range of relative density of 2.5 ± 0.01 g/cm^3 when sintered at 1500 °C, which was increased to 2.9 ± 0.01 g/cm^3 when sintered at 1600 °C, and further decreased to 2.7 ± 0.01 g/cm^3 when the sintering temperature reached 1700 °C. Moreover, the sample with intermediate amount of sodium ($Na_{1.71}Li_{0.33}Al_{10.67}O_{17}$) has the highest relative density at all sintering temperature with the maximum density of 3.0 ± 0.01 g/cm^3 when sintered at 1700 °C. Lifting up the sodium content to a certain amount to counterbalance Na_2O losses during sintering can promote the relative density of the ceramic, while excessive amount of sodium can further decrease the density.

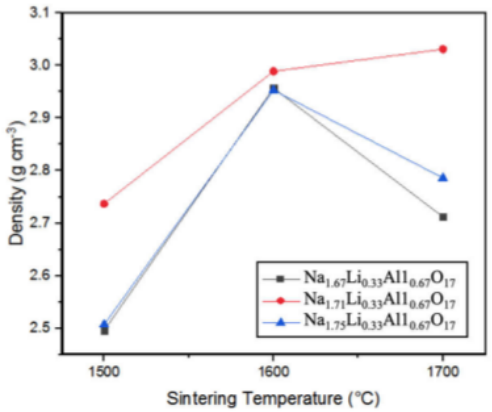

FIGURE 4. Density of Na-β”-alumina samples as a function of sintering temperature and sodium content.

XRD analysis

Fig.5a shows selection of XRD diffraction patterns of different sodium content and sintering temperature. The qualitative result shows the co-existence of Na-β”-alumina and sodium poor Na-β-alumina in accordance to database (PDF 84-0211 and PDF 25-0775, respectively). Moreover, lowly intensive peak of $NaAlO_2$ (PDF 33-1200) with a characteristic peak at 30.2° was detected. The quantitative phase composition was calculated by Rietveld refinement method (AutoQuan 2.8.0.2). The result is shown in **Fig.5b**. The increase of sintering temperature from 1500 until 1700 °C slightly increases the Na-β”-alumina phase content for samples with intermediate and high sodium content ($Na_{1.71}Li_{0.33}Al_{10.67}O_{17}$ and $Na_{1.75}Li_{0.33}Al_{10.67}O_{17}$, respectively). The increase of sintering temperature from 1500 to 1600 °C decreased the Na-β”-alumina phase content for the sample with low sodium content ($Na_{1.67}Li_{0.33}Al_{10.67}O_{17}$) from 54 to 35%. This might happened due to increase of Na_2O sublimation at higher sintering temperature [11]. Hence, the sodium poor Na-β-alumina phase was formed in exchange of Na-β”-alumina phase, as the amount of sodium was insufficient. In this work, the adjustment of sodium content to $Na_{1.71}Li_{0.33}Al_{10.67}O_{17}$ and sintering temperature of 1700 °C could result in Na-β”-alumina phase content of 83.8%.

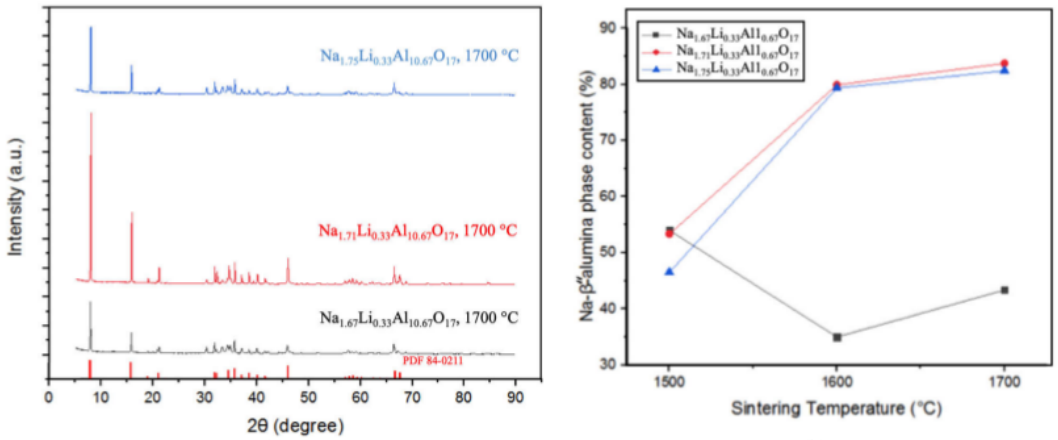

FIGURE 5. (a) XRD patterns of representative Li^+-stabilized Na-β"-alumina samples. The reflexes of PDF 84-2011 are shown at the bottom. (b) Na-β"-alumina phase content of the samples plotted against sintering temperature with different sodium contents.

Shan *et al.* reported Na-β"-alumina phase content for undoped sample of 54% [13]. Moreover, Dirksen *et al.* [14] reported Na-β"-alumina phase content in the range of 88.5-93.4% and Wei *et al.* [12] have reported the range between 95.2-98.1%. Both research groups synthesized titanium-doped Na-β"-alumina, which results in a significant increase of ionic conductivity. Hence, the result in this work is still in the range of previous studies.

Ionic conductivity analysis

For energy storage applications, high ionic conductivity electrolytes are targeted. In **Fig.6a**, the ionic conductivity of Na-β"-alumina ceramic samples with different sodium content are plotted against sintering temperature between 1500 and 1700 °C. The result displayed, that the ionic conductivity increases as the sintering temperature increased. The ionic conductivity of all samples was slightly lower when sintered at 1500 °C compared to samples sintered at 1600 °C, becoming almost negligible. At all sodium content, the highest ionic conductivity was achieved at sintering temperature of 1700 °C. The sample with tailored stoichiometry of $Na_{1.71}Li_{0.33}Al_{10.67}O_{17}$ and sintered at 1700 °C achieved the maximum ionic conductivity of 0.23 S cm^{-1}.

In addition, it can be seen that the measurement of samples $Na_{1.67}Li_{0.33}Al_{10.67}O_{17}$ and $Na_{1.75}Li_{0.33}Al_{10.67}O_{17}$ sintered at 1500 °C shows a wide range of results. Moreover, salt melt impregnated into the glass wool pad during measurement was completely absorbed to the sample pores. This might happened, as the samples are porous and not compactly sintered, which is accordance with SEM micrographs. Hence, this analysis method can be considered as not suitable for analyzing porous sample.

The measured conductivity in the temperature range between 240 until 330 °C are in good compliance with Arrhenius' equation. **Figure 6c** shows the activation energy for all prepared Li^+-stabilized Na-β"-alumina in this research. The activation energy obtained in this research lies between 0.17-0.24 eV, with the minimum value achieved by sample of $Na_{1.71}Li_{0.33}Al_{10.67}O_{17}$ and sintered at 1700 °C. The values were in compliance with previous research by Zhang *et al.* [7], where it is established that the ionic conductivity of Mg-SBA prepared through sol-gel method was 0.24 S cm^{-1} at 350 °C. Moreover, Butee *et al.* also reported the range of activation energy for Mg-stabilized Na-β"-alumina lies between 0.20-0.23 eV [5].

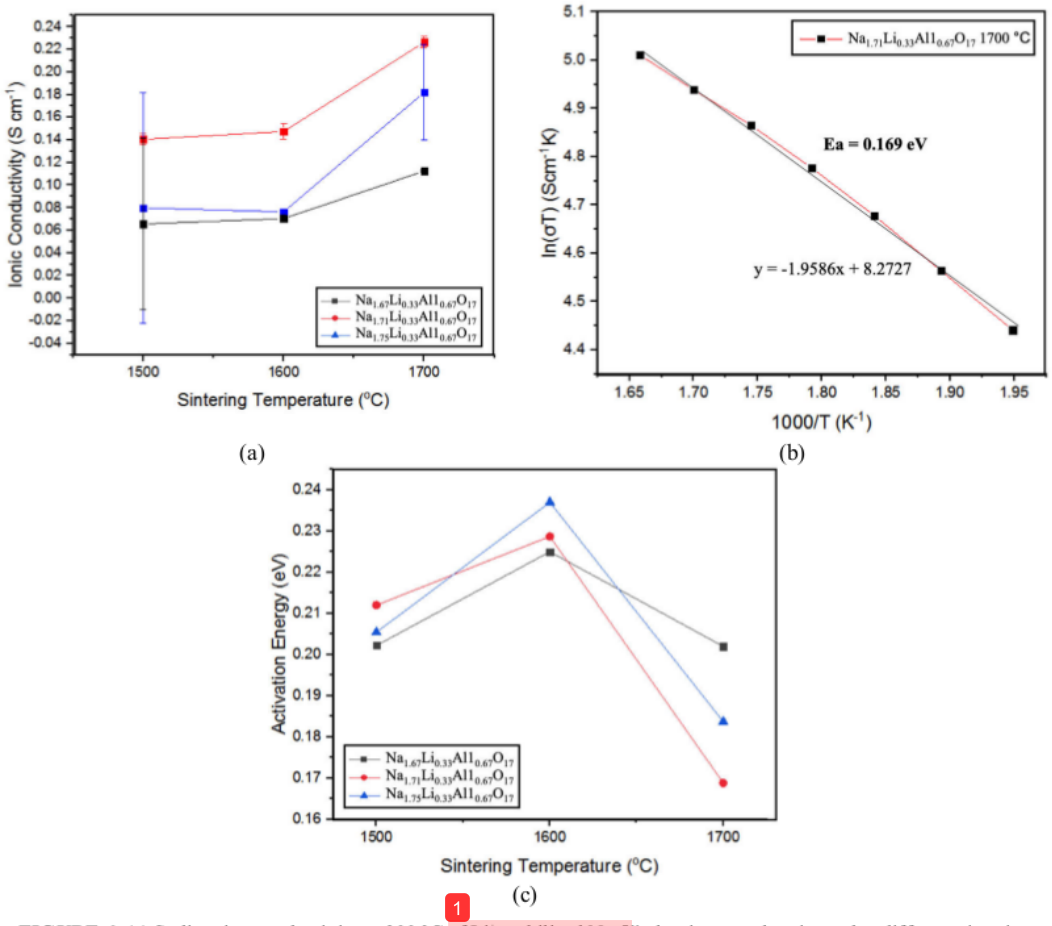

FIGURE 6. (a) Sodium ion conductivity at 300 °C of Li^+-stabilized Na-β"-alumina samples sintered at different sintering temperatures. (b) Arrhenius' plot from $Na_{1.71}Li_{0.33}Al_{10.67}O_{17}$ sample sintered at 1700 °C. (c) Activation energy of samples with different sodium contents plotted against sintering temperature.

Microstructure analysis

Impact of Sintering Temperature on Microstructure

The effect of sintering temperature to the microstructure of Na-β"-alumina solid electrolyte were evaluated by SEM images. SEM images of samples sintered at 1500 °C (**Fig.7**, left row), 1600 °C (**Fig.7**, middle row), and 1700 °C (**Fig.7**, right row) were compared. It is observed that sintering temperature of 1500 °C was not enough to compactly sinter the sample. Refinement in the grain size and compact materials can be observed in the samples sintered at 1600 °C. Moreover, it can also be seen that the grain size is gradually increasing as the sintering temperature increases. However, increasing amount of defects was also shown as another effect of higher sintering temperature when the sintering temperature reached 1700 °C. Defects presence is often cause by vacancy agglomeration due to high sintering temperature and extensive grain growth [14]. The presence of micro pores may also be possible due to increase of Na_2O sublimation (sublimation point at 1275 °C) [11]. Moreover, the increase of defects is corresponding well with the density analysis, which showed lower relative density at sintering temperature of 1700 °C.

Impact of Sodium Content on Microstructure

The microstructure of Na-β”-alumina solid electrolyte was also affected by the sodium content in the precursor. **Figure 7** shows samples with different sodium content, starting with the lowest and finish with the highest sodium content on the bottom. The least compact microstructure was shown by the samples with low and high sodium content ($Na_{1.67}Li_{0.33}Al_{10.67}O_{17}$ and $Na_{1.75}Li_{0.33}Al_{10.67}O_{17}$, respectively) at sintering temperature of 1500 °C, which shows a porous sample. This result was in accordance with the density measurement, as the samples shown relatively low density. Moreover, these samples showed more defects formation at all sintering temperature compared to sample with intermediate sodium amount sample ($Na_{1.71}Li_{0.33}Al_{10.67}O_{17}$). In addition, the $Na_{1.71}Li_{0.33}Al_{10.67}O_{17}$ sample shows a compact microstructure for all sintering temperature.

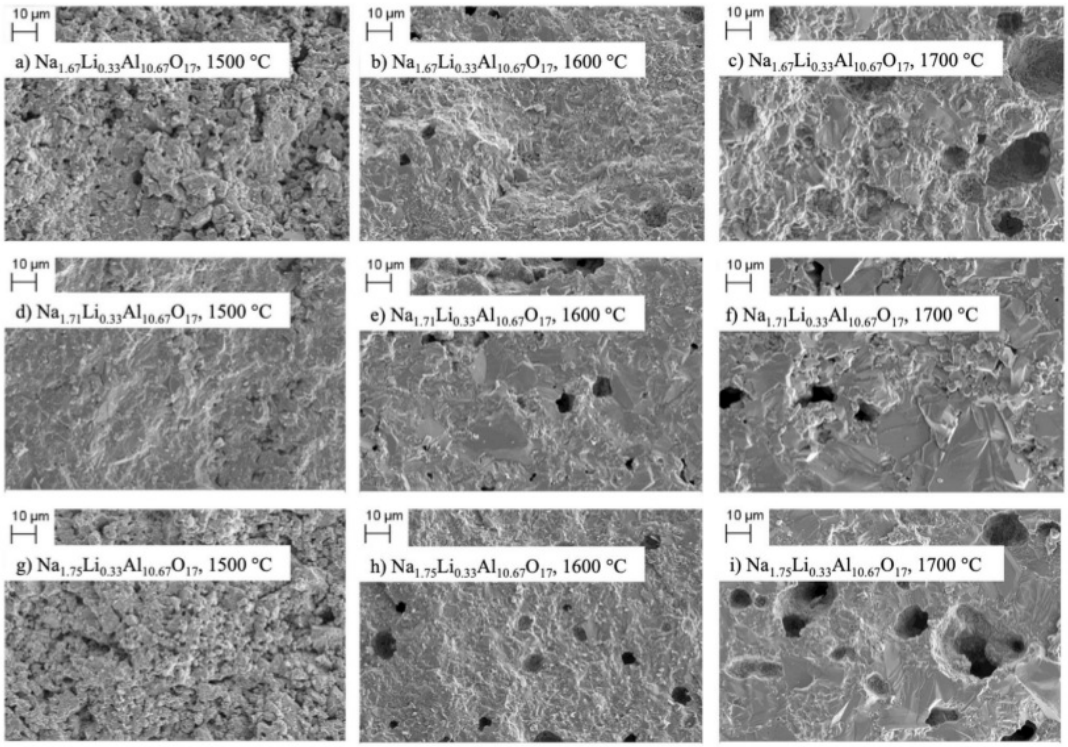

FIGURE 7. SEM images of Na-β”-alumina samples with different tailored stoichiometry and sintered at 1500 °C (left row), 1600 °C (middle row), or 1700 °C (right row).

CONCLUSION

In this research, Li^+-stabilized Na-β”-alumina with difference sodium content and sintered at three different temperatures were successfully synthesized through sol-gel based on *Pechini* method. The synthesis was done using citric acid and a small amount of ethylene glycol as the solvent stabilizer. The maximum ionic conductivity was 0.23 S cm^{-1} and a minimum activation energy of 0.17 eV with a tailored stoichiometry of $Na_{1.71}Li_{0.33}Al_{10.67}O_{17}$ at sintering temperature of 1700 °C. The highest relative density of 3.03 g cm^{-3} was also achieved by the same sample.

Hereby was also shown by XRD analysis that overall the samples exhibits Na-β”-alumina phase dominantly. Secondary Na-β-alumina and $NaAlO_2$ are also present in all samples, but adjustment of sodium content and sintering temperature could decrease the amount as low as 9.4 and 6.4% respectively. It is also established that insufficient amount of sodium could promote the formation of the sodium poor Na-β-alumina phase and excessive amount of

sodium could promote the $NaAlO_2$ phase formation. The adjustment of both parameters; sodium content and sintering temperature, can attribute to a change in microstructure.

ACKNOWLEDGMENTS

This work was cooperation between Fraunhofer Institute for Ceramics Technologies and Systems IKTS – Hermsdorf, Germany and Chemical Department of Swiss German University - Indonesia.

REFERENCES

1. S. Ha, J. K. Kim, A. Choi, Y. Kim, and K. T. Lee, "Sodium-metal halide and sodium-air batteries," *ChemPhysChem*, vol. 15, no. 10, pp. 1971–1982, 2014.
2. P. K. Nayak, L. Yang, W. Brehm, and P. Adelhelm, "From Lithium-Ion to Sodium-Ion Batteries: Advantages, Challenges, and Surprises," *Angew. Chemie - Int. Ed.*, vol. 57, no. 1, pp. 102–120, 2018.
3. G. Li *et al.*, "An Advanced Na-FeCl2 ZEBRA Battery for Stationary Energy Storage Application," *Adv. Energy Mater.*, vol. 5, no. 12, pp. 1–7, 2015.
4. G. E. Youngblood, G. R. Miller, and R. S. Gordon, "Relative Effects of Phase Conversion and Grain Size on Sodium Ion Conduction in Polycrystalline, Lithia-Stabilized β-Alumina," *J. Am. Ceram. Soc.*, vol. 61, no. 1–2, pp. 86–87, 1978.
5. S. Butee, K. Kambale, and M. Firodiya, "Electrical properties of sodium beta-alumina ceramics synthesized by citrate sol-gel route using glycerine," *Process. Appl. Ceram.*, vol. 10, no. 2, pp. 67–72, 2016.
6. A. V. Virkar, G. R. Miller, and R. S. Gordon, "Resistivity-Microstructure Relations in Lithia-Stabilized Polycrystalline β"-Alumina," *J. Am. Ceram. Soc.*, vol. 61, no. 5–6, pp. 250–252, 1978.
7. G. Zhang, Z. Wen, X. Wu, J. Zhang, G. Ma, and J. Jin, "Sol-gel synthesis of Mg2+ stabilized Na-β″/β- Al2O3 solid electrolyte for sodium anode battery," *J. Alloys Compd.*, vol. 613, pp. 80–86, 2014.
8. M. Pechini, "Method of Preparing Lead and Alkaline Earth Titanates and," 1967.
9. X. Lu, G. Xia, J. P. Lemmon, and Z. Yang, "Advanced materials for sodium-beta alumina batteries: Status, challenges and perspectives," *Journal of Power Sources*, vol. 195, no. 9. pp. 2431–2442, 2010.
10. J. L. Sudworth, "The sodium/sulphur battery," *J. Power Sources*, vol. 11, no. 1–2, pp. 143–154, 1984.
11. J. D. Hodge, "Phase Relations in the System Na2O-Li2O-Al2O3," *J. Am. Ceram. Soc.*, vol. 67, no. 3, pp. 183–185, 1984.
12. X. Wei, Y. Cao, L. Lu, H. Yang, and X. Shen, "Synthesis and characterization of titanium doped sodium beta″-alumina," *J. Alloys Compd.*, vol. 509, no. 21, pp. 6222–6226, 2011.
13. S. J. Shan, L. P. Yang, X. M. Liu, X. L. Wei, H. Yang, and X. D. Shen, "Preparation and characterization of TiO2 doped and MgO stabilized Na-β″-Al2O3 electrolyte via a citrate sol-gel method," *J. Alloys Compd.*, vol. 563, pp. 176–179, 2013.
14. C. L. Dirksen, K. Skadell, M. Schulz, and M. Stelter, "Effects of TiO 2 doping on Li + -stabilized Na-B″-alumina for energy storage applications," *Sep. Purif. Technol.*, vol. 213, pp. 88–92, 2019.

Anisa Isabella

ORIGINALITY REPORT

3%	1%	3%	1%
SIMILARITY INDEX	INTERNET SOURCES	PUBLICATIONS	STUDENT PAPERS

PRIMARY SOURCES

1	Marie-Claude Bay, Meike V. F. Heinz, Renato Figi, Claudia Schreiner et al. "Impact of liquid phase formation on microstructure and conductivity of Li-stabilized Na-β''-alumina ceramics", ACS Applied Energy Materials, 2018 Publication	<1%
2	Li-Ping Yang, Shi-jie Shan, Xiao-ling Wei, Xiao-min Liu, Hui Yang, Xiao-dong Shen. "The mechanical and electrical properties of ZrO2–TiO2–Na-β/β″-alumina composite electrolyte synthesized via a citrate sol–gel method", Ceramics International, 2014 Publication	<1%
3	Lukas Medenbach, Pascal Hartmann, Juergen Janek, Timo Stettner et al. " A Sodium Polysulfide Battery with Liquid/Solid Electrolyte: Improving Sulfur Utilization Using P S as Additive and Tetramethylurea as Catholyte Solvent ", Energy Technology, 2020 Publication	<1%

www.inderscience.com

4	Internet Source	<1%
5	Chengtian Zhou, Sourav Bag, Venkataraman Thangadurai. "Engineering Materials for Progressive All-Solid-State Na Batteries", ACS Energy Letters, 2018 Publication	<1%
6	doaj.org Internet Source	<1%
7	Kuo, C.K.. "Equilibrium calculations in the gas participating multicomponent system", Physica B+C, 198805 Publication	<1%

Exclude quotes	On	Exclude matches	< 10 words
Exclude bibliography	On		